

Imidazoline Derivatives Based on Coffee Oil as CO₂ Corrosion Inhibitor

J. Porcayo-Calderon^{1,2,*}, L.M. Martínez de la Escalera³, J. Canto³, M. Casales-Diaz²

¹ Universidad Autonoma del Estado de Morelos, CIICAp, Av. Universidad 1001, 62209-Cuernavaca, Morelos, Mexico

² Universidad Nacional Autonoma de Mexico, Instituto de Ciencias Fisicas, Av. Universidad s/n, Cuernavaca, Morelos, Mexico

³ Corrosion y Proteccion, Buffon 46, Mexico City, C.P. 11590, Mexico

*E-mail: jporcayoc@gmail.com

Received: 8 January 2015 / Accepted: 6 February 2015 / Published: 24 February 2015

In this work, a hydroxyethyl-imidazoline derivate based on coffee oil has been synthesized and evaluated as an inhibitor of corrosion for carbon steel in CO₂-saturated (3% NaCl + 10% diesel) emulsion at 50°C. Electrochemical impedance spectroscopy has been used to study the film formation on carbon steel. Performance of inhibitor was evaluated by adding 0, 5, 10, 25, 50, and 100 ppm. EIS data were used to calculate corrosion related electrochemical parameters, and this technique was shown to be a very useful tool for studying corrosion inhibitors. Optimal concentration is 10 ppm, by decreasing the corrosion rate by over 99.9%. Lower or higher concentrations increases the corrosion rate because the surface area covered by the inhibitor decreases, causing the formation of unprotected sites on the metal.

Keywords: Green inhibitor, NaCl corrosion, acidic corrosion, imidazoline, coffee oil

1. INTRODUCTION

Corrosion is the destructive phenomenon which affects almost all metals, and iron is the most widely used metal. Three main reasons for the importance of corrosion are economics, safety and conservation. Where the economic impact can be reduced by reducing material losses, safety must be a critical consideration in equipment design, and protection techniques should contribute to the conservation of equipment and structures to minimize the loss of metal by corrosion and the cost of rebuilding. The costs associated with corrosion cannot be eliminated entirely and it is impossible to completely prevent corrosion. Therefore the most economical solution is to control the rate of the corrosion.

The corrosion inhibition in oil and gas field is complicated and requires specialty inhibitors depending on the area of application such as in refineries, wells, recovery units, pipelines etc. Where the presence of aggressive gases such as H_2S , CO_2 complicate the problem of inhibition. With the exploitation of oil and gas well containing carbon dioxide, CO_2 corrosion has become one of the universal problems in the oil and gas industries responsible for lost production and expensive repairs. It occurs at all stages of production from downhole to surface equipment and processing facilities. Corrosion inhibitors have been considered as the first line defense against internal corrosion of pipelines. In conjunction with the use of carbon steel, corrosion inhibitors have been recognized as the most practical and cost-effective option. There are two types of CO_2 corrosion inhibitors used in oil and gas industry. Inorganic inhibitors such as chromate and nitrate, which form a film onto surface acting as a barrier against the aggressive species, however the disadvantages of inorganic inhibitors are that they are required in large dosages, apart from their unsatisfactory effectiveness. Organic inhibitors are adsorption-type inhibitors which reduce corrosion rate by forming layers of hydrophobic film onto metal surface, which hinders the transport of aggressive species and charges related to electrochemical reactions. The most widely used are the nitrogen-containing compounds, for example amines, amides, quaternary ammonium salts, imidazolines and their derivatives, salts of nitrogenous molecules with carboxylic acids, polyoxyalkylated nitrogen-containing compounds, nitrogen heterocyclics and compounds containing phosphorus, sulfur and oxygen [1-9]. These inhibitors are categorized as surfactants due to their amphiphatic, lipid-like molecular structure. However, usually in hydrocarbon pipelines, inhibitors are injected into the stream which causes the inhibitor to stay with the liquid at the bottom of the line, making the top line more vulnerable to corrosion [10].

Nitrogen-based organic compounds, such as imidazoline and its derivatives, have been used successfully to protect mild steel in oil and gas wells and pipelines from carbon dioxide (CO_2) and hydrogen sulfide (H_2S) corrosion [1-9]. These organic compounds inhibit the corrosion of mild steel by adsorption on the metal-solution interface thereby creating a barrier that prevents the active ions in the corrosion reactions to get to the surface. However, despite extensive use of imidazoline corrosion inhibitors the mechanism of inhibition remains poorly understood. Therefore, in order to develop more cost-effective inhibitors, a better understanding of the mechanism of inhibition of current and new inhibitors is needed [11].

In the search for sustainable sources, great interest has been aroused about the use of renewable raw materials in order to exploit the synthetic capabilities of nature. Oils and fats from vegetable and animal origin are the greatest proportion of the current consumption of renewable raw materials in the chemical industry, since they offer to chemistry a large number of possibilities for applications. However, future progress will be along the lines of the use both waste or by-products agro-industrial as sources of vegetable fats and oils. This in order not to affect the food sources for human consumption. Such progress is essential for a growth in the use of oils and fats as renewable raw materials. This it is an important advantage not only in terms of sustainability, but also in terms of industrial feasibility. The chemistry processes that can be applied to fatty acids is reflected on the large amount of publications dealing with the use of fatty acids in the synthesis of valuable derivatives [21-28].

In this regard, it is known the use of coffee oil as feedstock for biofuels. However, to date it has not been reported the use of imidazoline derived from coffee oil as corrosion inhibitors. The coffee

waste resulting from the preparation of coffee drinks and other products based on coffee grain have a content of 13-15% oil (dry basis), which includes the linoleic acid as the most abundant fatty acid. Linoleic acid is doubly unsaturated, which gives to the coffee oil based imidazolines an enhanced adhesion to the metal surfaces. Thus, it was considered interesting to synthesize imidazoline derivatives based on coffee oil where the coffee oil used for the synthesis was extracted from coffee bagasse, and to assess their inhibitive properties in a CO₂-saturated (3% NaCl + 10% diesel) emulsion at 50°C. Evaluation was carried out by electrochemical impedance spectroscopy (EIS) which has already been successfully used in various corrosion and protection fields. This technique can provide information on the corrosion and protection mechanisms as for example, when an adsorbed film is present. EIS data can be used to calculate corrosion related electrochemical parameters to understand the performance of the corrosion inhibitors.

2. EXPERIMENTAL PROCEDURE

The chemical composition (wt.%) of 1018 carbon steel used was 0.190 C, 0.670 Mn, 0.0003 P, 0.001 S, and balance Fe. Before the tests, cylindrical specimens (4.55 cm length, 0.63 cm diameter) were ground to 600 grade emery paper then first rinsed with distilled water and later by ethanol in an ultrasonic bath for 10 minutes. Specimens with this surface condition were employed as the working electrode (WE) in the electrochemical tests.

Inhibitors used in this work were hydroxyethyl-imidazoline derivative based on coffee oil. Coffee oil used for the synthesis of the inhibitors was extracted from coffee bagasse. General procedure for the synthesis of the imidazoline derivatives based on coffee oil is similar to that detailed elsewhere [6]. The inhibitors were dissolved in pure 2-propanol. The concentrations of the inhibitor used in this work were 5, 10, 25, 50 and 100 ppm. Testing solution consisted in a CO₂-saturated (3% NaCl + 10% diesel) emulsion, heated, de-aerated by purging with CO₂ gas during 2 hours prior the experiment and kept bubbling throughout the experiment. The electrochemical cell used was that described by standard ASTM G5 and shown on figure 1.

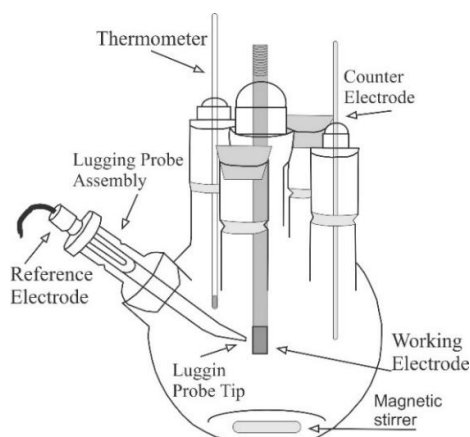


Figure 1. Experimental set-up for electrochemical measurements

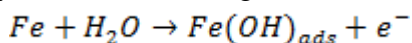
Test temperatures was 50°C. For each electrochemical test a volume of 600 ml of fresh solution was used. Electrochemical technique employed was electrochemical impedance spectroscopy (EIS) measurements. Measurements were obtained by using a conventional three electrodes glass cell. A saturated calomel electrode (SCE, 0.242V vs. SHE) was used as the reference electrode with a Luggin capillary bridge, and a high density and high surface area graphite rod was used as the counter electrode. All impedance data were recorded under open-circuit conditions using a sinusoidal excitation voltage of 10 mV, and a frequency interval of 0.01-100 KHz. A model PC4 300 Gamry potentiostat was used. After testing, corroded specimens were analyzed in a DSM 960 Carl Zeiss scanning electronic microscope (SEM).

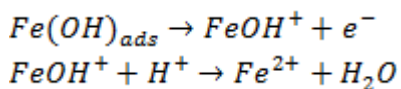
3. RESULTS AND DISCUSSION

Bode plots for carbon steel exposed to CO₂-saturated (3% NaCl + 10% diesel) emulsion at 50°C is shown on figure 2. In general, three frequency regions referring to the high, intermediate and low frequency values are observed from Bode diagrams [12]. In the high frequency region the log |Z| values tend to a constant where the phase angle approaches zero. The constant value observed correspond to the solution resistance (R_s).

In the intermediate frequency region, there is a linear relationship between log |Z| and log f , the slope value is lower than -1, and phase angle value less than 90°. This indicates that the developed oxide layer has not a capacitive nature and that the corrosion process can be under mixed control (diffusion and charge transfer). It is observed the presence of a single phase between 10-30 Hz, which is shifting to lower frequencies as time elapses, and this change was associated with a slight increase of the phase angle and with a steady decrease in the slope of the log |Z|-log f relation. The displacement of the spectrum of phase angle toward lower frequencies, it may be associated with detachment, or thinning of the protective films [7, 22].

This is consistent with that observed in the low frequency region, in this region as time elapses, the maximum values observed in the plateau region show a slight tendency to decrease which confirms an active corrosion process. This is evidence of the non-protective nature of the corrosion products. The main formed film during CO₂ corrosion of carbon steels is iron carbonate, FeCO₃. Thus, it seems that FeCO₃ scale is not fully formed on the steel surface, and therefore the corrosion rate shows a slight increases. From Nyquist diagrams (not showed) could be observed that in the high and intermediate frequency values, the data describes a depressed, capacitive-like semicircle, with its center at the real axis, indicating that the corrosion process is under charge transfer control from the metal surface to the environment through the double electrochemical layer. As time elapses, the high-intermediate frequency semicircle diameter decreases, increasing the corrosion rate, showing the non-protective nature of the corrosion products. However, at lower frequency values, both the scattering of experimental points and the contraction of Z_{re} , forming an inductive loop were evident. This phenomena has been associated to the adsorption of intermediate species as FeOH due to the hydrolysis of Fe according to [23]:





Also, some authors suggest that this is typical of mass-transfer controlled processes [24]. This means that the adsorption of intermediate species (FeOH) is favoring the occurrence of diffusional processes, where the diffusional process can be of three different types [25]. The first one happens when the thickness of stagnant layer is infinite and it called semi-infinite diffusion process (Warburg diffusion), the second one it is a transmissive finite diffusion process with real part contraction and its happen when the thickness of the stagnant layer is finite, and the third one is a reflective finite diffusion process, which happens when only the transmission takes place in a limited distance. Accordingly, the presence of intermediate species cause a finite transmissive diffusion process.

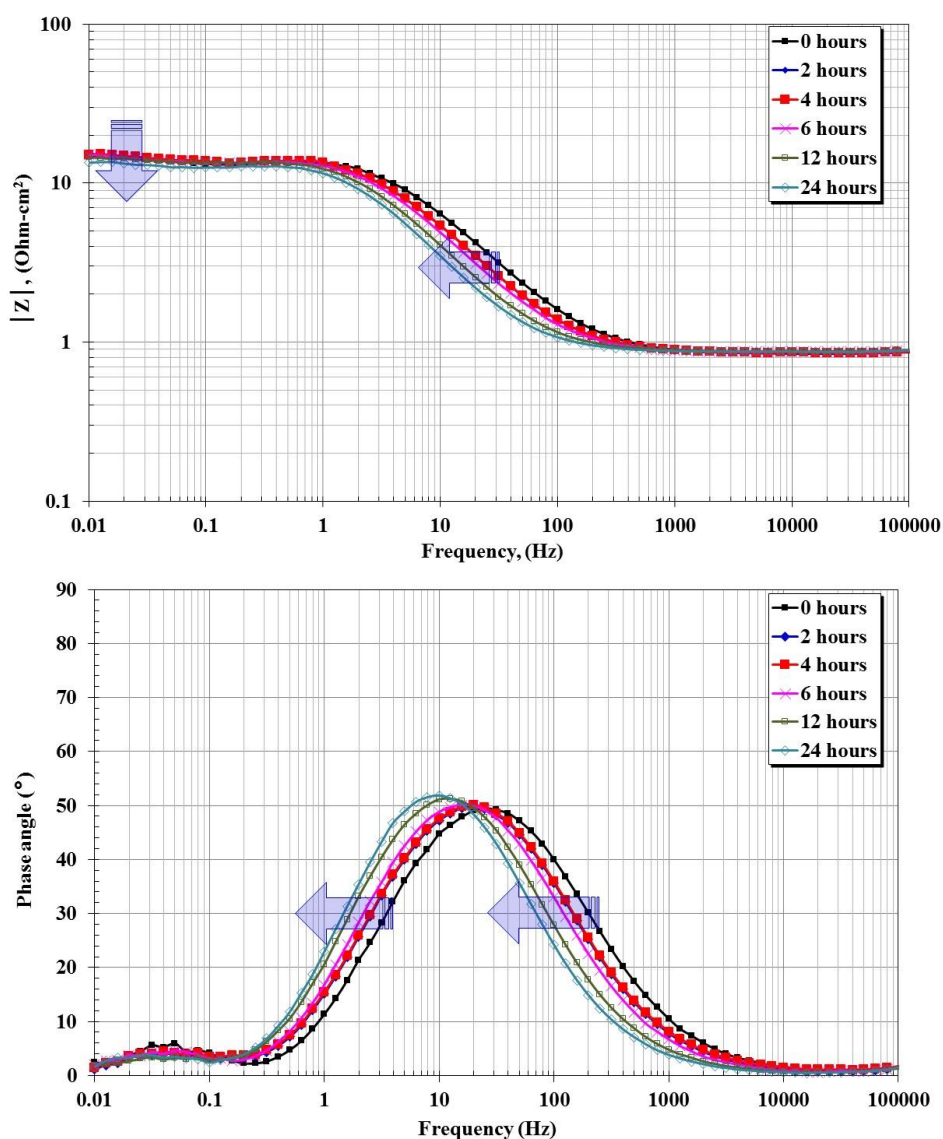


Figure 2. Bode plots for 1018 carbon steel in CO₂-saturated (3% NaCl + 10% diesel) emulsion without inhibitors at 50°C.

Figure 3 shows the Bode plots for carbon steel exposed in the CO₂-saturated (3% NaCl + 10% diesel) emulsion with 10 ppm of inhibitor at 50°C. Similar behaviors were obtained with the other concentrations. Figure 4 shows the Nyquist and Bode plots with different additions of inhibitor after 24 hours of test. From this figures, in all cases it was observed as time elapse that in the high frequency range the plateau region begins to form at higher frequencies than 100,000 Hz, i.e., in the frequency range under study the log |Z| values do not tend to a constant. At the same time, the phase angle-frequency relationship shows the evolution of a new loop and its value increases over time. It is known that the Bode plot exhibits a plateau (horizontal line) of the log |Z| values at $f > 10^3$ Hz, with the phase angle approaching 0°, and this is the characteristic impedance response of the electrolytic resistance (resistive region), yields the value of the solution resistance, R_s [21, 26]. However, in this case the formation and evolution of the new loop is owing to the formation of self-assembled inhibitor films on the carbon steel surface. In solutions without inhibitor, the corrosion of the carbon steel provokes the dissolution (Fe²⁺) of the bare metal and its reaction to form a non-passivating porous adherent corrosion product that does not interferes with the access of the electrolyte to the metal surface, and in this case, the response observed is that of the figure 2. However, in inhibited solutions the model for corrosion inhibition by oleic imidazolines suggests a series of surface processes involving a strong bonding by the imidazoline head group to the metal surface through the electron pair of nitrogen of imidazoline ring, followed by a self-assembly of the head groups to form a dense ordered overlayer, and a self-organization of the tails to form a dense tightly packed hydrophobic film that serves as a barrier for migration of the corrosive species to the metal surface, including water, oxygen, and electrons [27]. But it should be noted that this barrier formed by the inhibitor film is not a solid layer (nor free of imperfections), on the contrary, it is a layer of oily nature and therefore its formation is detected in the high frequency region. The protective ability of the inhibitor molecules depend on its solubility and rate of transport toward the surface of the carbon steel. It has been showed that the process of adsorption to the imidazoline-type inhibitors is enhanced by the reduction in the pH of the solution due to the presence of CO₂ causing both an increase of solubility and stability of the inhibitor [22]. This is important owing that the imidazoline compounds are susceptible of hydrolysis in aqueous-basic media, but at pH < 6 its hydrolysis is not virtually observed, because drastic conditions are necessary in order to decompose the imidazoline structure [28]. Thus the inhibitor can reach the steel surface and not to be absorbed onto the water-soluble fractions (WSF's) of the diesel. It is observed that the phase angle maximum value increases and shifts to higher frequencies as time elapses. The maximum value of the phase angle was 75 ° at 10,000 Hz. This suggests an increase in the thickness of the inhibitor film formed on the surface of carbon steel and an increase in its protective ability.

In the intermediate frequency region, there is a linear relationship between log |Z| and log f, and only one slope is observed. The values of slopes are higher than those observed in the uninhibited solution, indicating that the layers formed onto steel surface are more protective than those developed in the uninhibited solution (figure 2). Phase angle-frequency relationship also shows the presence of one loop and its maximum value increases in the first two hours and thereafter tends slightly to decrease. Only at 100 ppm its maximum value increases as time elapses. On the other hand, a shift to lower frequencies of the intermediate loop from 30 Hz at 5 Hz is observed. Only at 5 ppm the loop shows a shift to lower frequencies, and then returned at intermediate frequencies. The presence of this

loop indicates both the formation and evolution of the corrosion products layer. In this case, the displacement of the spectrum of phase angle toward lower frequencies may be associated with the thinning of the corrosion products layer owing the protective action of the inhibitor [7, 22].

On the other hand, in all cases in the low frequency region, the $\log |Z|$ values tend to a constant and the phase angle approximates to zero. Impedance module ($|Z|$) was increased to three orders of magnitude compared to those for uninhibited solution. However, unlike the uninhibited solution, the maximum impedance module ($|Z|$) obtained does not reach a final steady value, that is, the modulus of impedance ($|Z|$) can be increased to longer test times. This indicates the protective nature of the inhibitor film formed onto carbon steel surface. However, the maximum value reached was independent of the concentration of added inhibitor. As time elapsed, phase angle trends to zero at frequencies below 0.01 Hz, and a scattering in the experimental data is observed. It has been suggested that this type of behavior is because there is a transmissive finite diffusion process and it happen when the thickness of the stagnant layer onto steel surface is finite [25].

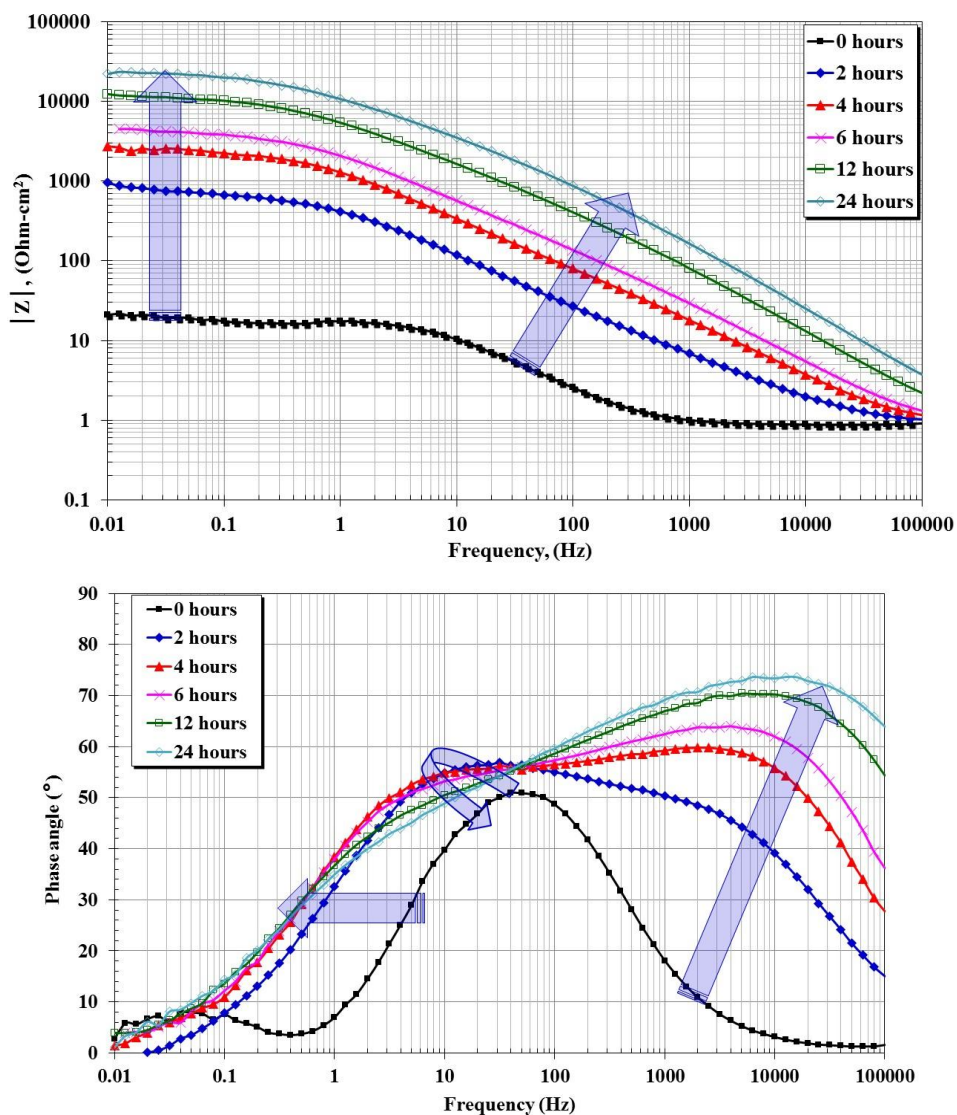


Figure 3. Bode plots for 1018 carbon steel in CO₂-saturated (3% NaCl + 10% diesel) emulsion with coffee oil derivate inhibitor (10 ppm) at 50°C.

This behavior it is owing the presence of the inhibitor film onto the steel surface, where the long hydrocarbon chains are responsible for their capacity of forming protective barriers against aggressive ions from the bulk solution.

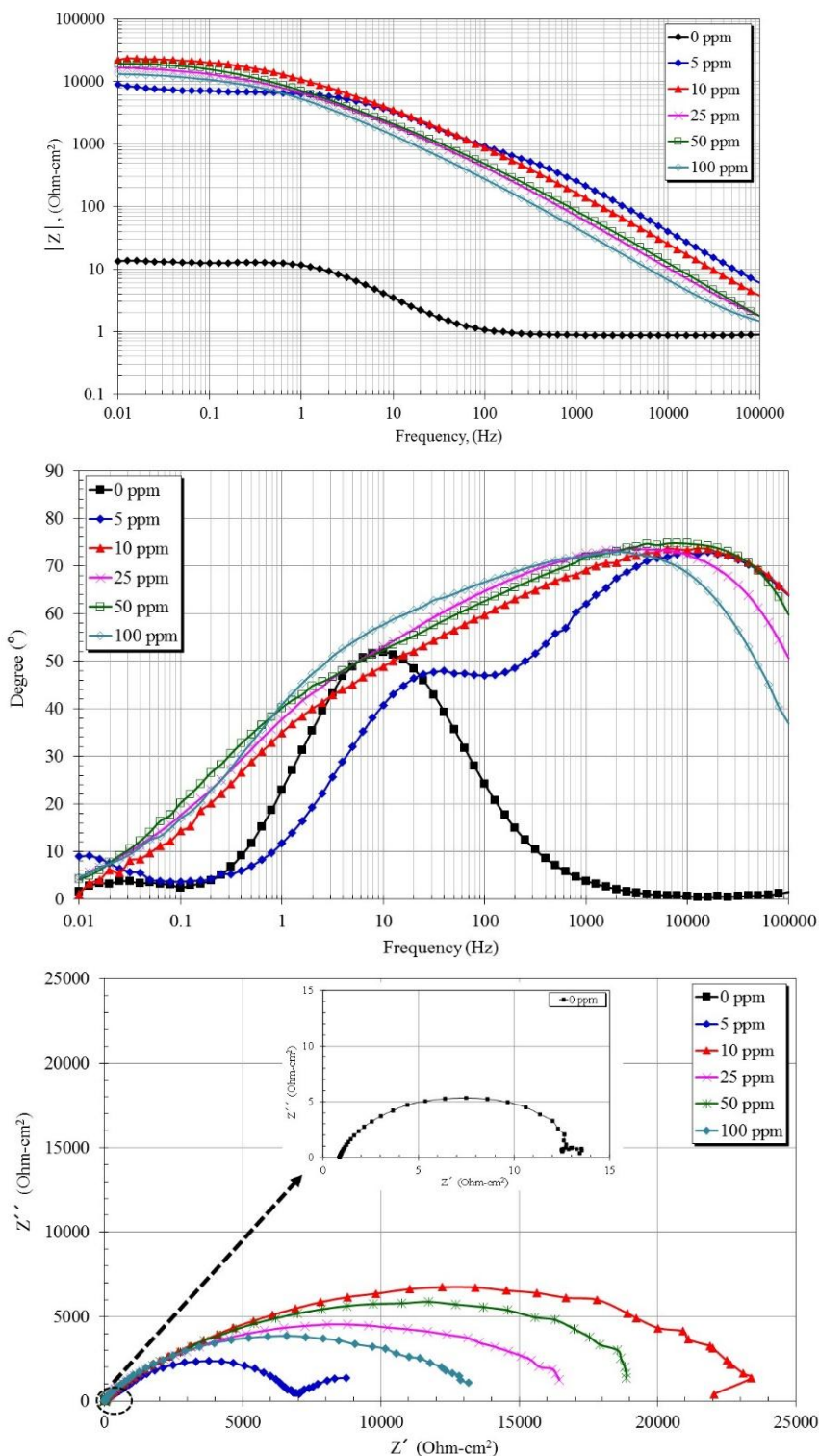


Figure 4. Nyquist and Bode plots for 1018 carbon steel in CO₂-saturated (3% NaCl + 10% diesel) emulsion with different additions of inhibitor after 24 hours.

In the low frequency region the electron charge transfer processes, the mass transfer processes, or other relaxation processes taking place at the film-electrolyte interface or within the pores of the surface film are detected. According to the results shown in Figure 4, the order of efficiency was; 10 ppm > 50 ppm > 25 ppm > 100 ppm > 5 ppm > 0 ppm. This behavior is due to the packing efficiency of the molecules of the inhibitor onto metal surface. When the inhibitor is not in sufficient concentrations there are unprotected sites, but when it is present in excess, it is possible the occurrence of electrostatic repulsion forces which prevent an efficient packaging causing the appearance of unprotected sites onto metal surface.

3.1. Surface morphology

Nevertheless that the electrochemical methods are useful in studying corrosion processes, alone do not provide the information in order to elucidate the mechanisms of the system under study. It has been suggested the use of complementary techniques, i.e., scanning electron microscopy (*SEM*), auger electron spectroscopy (*AES*), among other, in order to clarify both the morphology of the attack as well as the chemical composition and the elements distribution. Combination of these methods provides the information to understand the reactions occurring on the surface [29]. Therefore the superficial aspect of the working electrodes was studied using *SEM* in order to defining the morphology of the attack caused by the aggressive species present and the effect of adding the inhibitor at different concentrations.

The surface morphologies of carbon steel in CO₂-saturated (3% NaCl + 10% diesel) emulsion in the absence and presence of the inhibitor are presented in figure 5. From figure, it is clear that the surface morphology of carbon steel evaluated in absence of inhibitor (0 ppm) shows a rough appearance due to a rapid corrosion attack. Presence of pits greater than 50 microns was detected. The type of attack was of generalized corrosion with localized attack (pitting). However, when the inhibitor is added, the surface appearance of the carbon steel depend on the amount of inhibitor added. With the addition of 5 ppm of inhibitor, a surface with few surface damage but with the presence of localized attack is observed. This might be because the amount of added inhibitor was insufficient to form a protective film on the carbon steel surface. However with the addition of 10 ppm of inhibitor, a uniform surface without pitting attack is observed. In this condition only uniform corrosion was detected, and it is possible observe the lines generated by the grinding process. However, by adding both 25 and 50 ppm of inhibitor, a big density of pits on the surface is observed. Pitting attack was favored at these concentrations of inhibitor. Moreover, with the addition of 100 ppm of inhibitor, a similar surface morphology to that obtained with the addition of 10 ppm was observed. However, the presence of some areas with small pitting was also detected. It can be noticed that the effect of the inhibitor is different depending upon its concentrations. This can be because when the adsorbed inhibitor molecules exceed certain number onto the surface, these molecules are close enough, and electrostatic repulsion can occur between them, leading to a desorption of the inhibitor molecules. This electrostatic repulsion can causes the appearance of unprotected sites on the metal, which may be the

routes that led the pitting attack observed. According to the evidence of morphological analysis, the most efficient inhibitor concentration is 10 ppm.

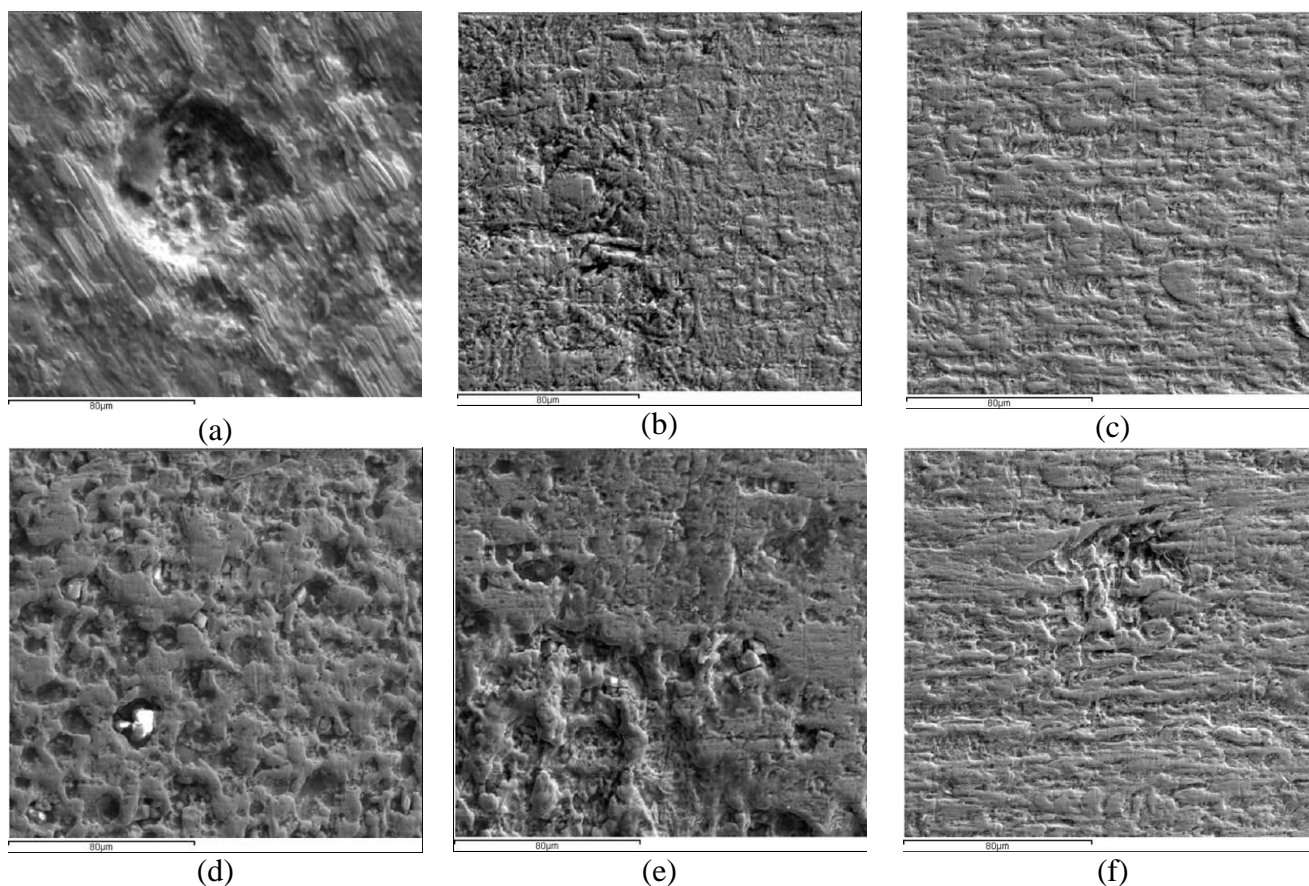


Figure 5. Corrosion morphology of carbon steel in CO_2 -saturated (3% NaCl + 10% diesel) emulsion with the addition of coffee oil derivate inhibitor at different concentrations, (a) 0 ppm, (b) 5 ppm, (c) 10 ppm, (d) 25 ppm, (e) 50 ppm, and (f) 100 ppm.

3.2. Analysis of impedance data

In order to interpret the electrochemical behavior of a system from *EIS* spectra, it is necessary an appropriate physical model of the electrochemical reactions occurring at the electrode surface. Through the analysis of the spectra of *EIS* and the surface analysis of the working electrodes by *SEM*, it is possible to define the appropriate equivalent circuit in order to analysis the impedance data. Equivalent circuits are used to model the electrochemical behavior and calculate the parameters of interest, such as electrolyte resistance (R_s), charge transfer resistance (R_{ct}), and double layer capacitance (C_{dl}). However, when a non-ideal frequency response is present, it is accepted to employ distributed circuit elements in an equivalent circuit. The most widely used is the constant phase element (*CPE*), which has a non-integer power dependence on the frequency. *CPE* is used in a model in place of a capacitor to compensate the inhomogeneity in the system which takes into account the irregularities of the surface such as roughness or because properties such as double layer capacitance,

charge transfer rate are non-uniformly distributed. The so-called *CPE* is an element whose impedance value is a function of the frequency and whose phase is independent of the frequency and its impedance is defined as:

$$Z_{CPE} = \frac{1}{Y_0} (i\omega)^{-n}$$

where Y_0 is a proportional factor that indicates the combination of properties related to both the surfaces and electroactive species independent of frequency; i is imaginary number ($\sqrt{-1}$); ω is the angular frequency and equal to $2\pi f$, where f is the frequency; and n has the meaning of a phase shift and is related to a slope of the $\log |Z|$ vs. $\log f$ plots and usually is in the range 0.5 and 1. When the value of n is equal to 1, the *CPE* describes an ideal capacitor with Y_0 equal to the capacitance. For $0.5 < n < 1$ the *CPE* describes a distribution of dielectric relaxation times in frequency space, and when n is equal to 0.5 the *CPE* represents a Warburg impedance with diffusional character. In these situations the semicircle in the *Zre-Zim* spectra is more and more depressed and the depression degree depends on the phase of the *CPE* [30]. The impedance plots can be analyzed according to the electric equivalent circuits given in figure 6 [22]. According to results for metal electrodes corroded without the presence of inhibitor there is one peak in the phase angle vs. frequency plot, indicating only one time constant (Figure 2), and this one is related to the corrosion process at the metal/corrosion products/electrolyte interphase. It can be modelled by a simple Randles equivalent circuit (Figure 6a) which allows to calculate both the electrolyte resistance (R_s), the charge transfer resistance (R_{CT}) and double layer capacitance (Z_{CPE}). On the other hand, for metal electrodes corroded in presence of inhibitor, from phase angle vs. frequency plot, two separate peaks can be clearly seen indicating the existence of two time constants (Figures 3 and 4). Where the high frequency time constant indicates the presence of an inhibitor film covering the surface, and the intermediate and low frequency one is related to corrosion process at the unprotected sites of the metal surface. In this case, the time constants can be modelled by the equivalent circuit showed in Figure 6b. The equivalent electrical circuit represent a porous inhibitor film formed onto the metal surface, in which Z_{CPEf} is related to the non-ideal capacitance of the inhibitor film, R_f to the inhibitor film resistance, which reflects the protective properties of the inhibitor film, and Z_{CPEdl} to the non-ideal capacitance of the double layer of the electrolyte/corrosion products/metal interphase. In this case, $R_f < R_{ct}$, hence $Y_0 = Y_f + Y_{dl} \sim Y_{dl}$. [4, 22, 31]. The evolution of the fitting parameters obtained using the electrical circuits shown in Figure 6 are presented in Figures 7 to 9.

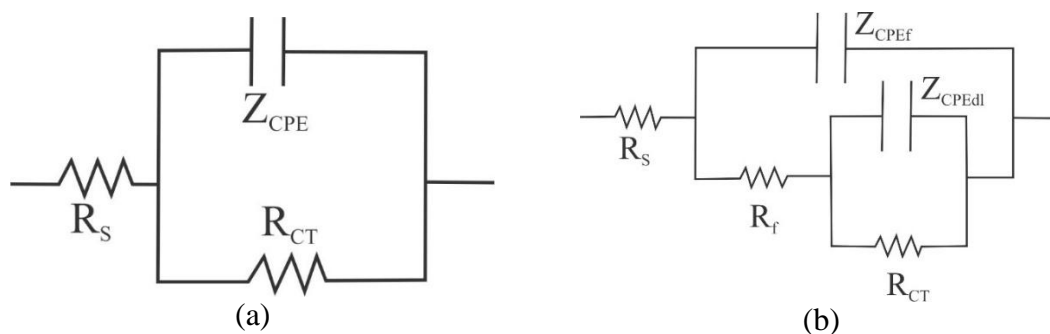


Figure 6. Equivalent circuits; (a) CO₂-saturated (3% NaCl + 10% diesel) emulsion without inhibitor; (b) CO₂-saturated (3% NaCl + 10% diesel) emulsions with inhibitor.

Figure 7 shows the variation of R_{ct} and R_f for each simulated condition. From R_{ct} plot can be seen that 1018 carbon steel showed the lowest corrosion resistance. On the other hand, its R_{ct} values tend to slightly decrease as time elapse. This is because the corrosion product layer was not protective notwithstanding that the presence of CO_2 dissolved causes an increase in the corrosion resistance of the carbon steel. However at 50 °C, these scales are porous and nonhomogeneous, allowing the access of the corroding solution to the base material [4]. It seems that the FeCO_3 film increased in thickness reaching a maximum value and after it was detached from the steel surface or it was thinned by some dissolution process. However, as soon as the inhibitor is added, regardless of the inhibitor concentration, it can be seen that the corrosion resistance of the carbon steel is increased until three orders of magnitude. An abrupt increase to two orders of magnitude in the R_{ct} values are observed in the first two hours of immersion. This indicates that regardless of the concentration of added inhibitor, the inhibitor immediately begins to form a protective film onto the carbon steel surface. Thereafter R_{ct} values tend to increase continuously without reaching the steady state. The observed increase in the R_{ct} values of up to three orders of magnitude indicating an efficiency protection of the 99.9%. In this case, the protective nature of the film-formed inhibitor can be explained only with an adsorption process. In general, it is known that the molecular structure of oil-based imidazolines, are composed of a five-member ring containing nitrogen elements, a hydrophobic head group, and a pendant, hydrophilic group attached to one of the nitrogen atoms. And this compounds can be adsorbed on the metal surface owing the formation of a Fe-N coordination bond and due a pi-electron interaction between the pi-electron in the head group and Fe. Moreover, although it is not the main contribution to the adsorption strength of the imidazoline compounds onto the metal surface, the coulombic attraction between the negative charges, i.e. electrons, on the surface of the metal and the inhibitor may also contribute to the inhibitory capacity of the imidazoline compounds [23]. On the other hand, the R_f values observed are lower respect those of R_{ct} . This is consistent because the inhibitor-adsorbed film is not solid film, but rather it is an oily film of a few angstroms thick, and therefore the formation of the inhibitor film will always be detected in the high frequency region. However, this adsorbed film has a high capacity to prevent the diffusion of aggressive species through it.

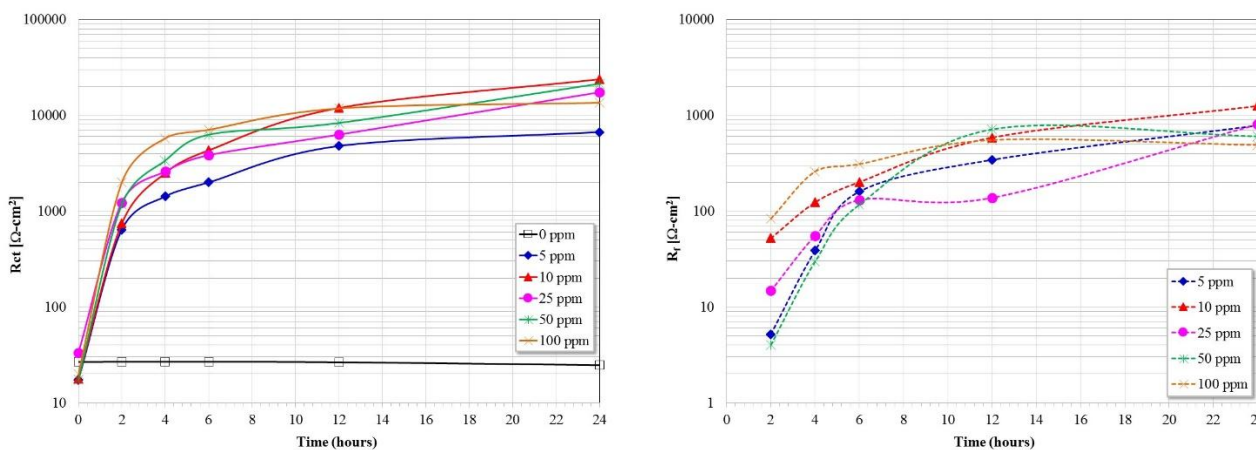


Figure 7. R_{ct} and R_f variation against time for carbon steel at different concentrations of coffee oil imidazoline.

In this regard, from Figure 8, the n_{ct} and n_f variation against time at different concentrations of inhibitor is observed. It is said that when the value of n is equal to 1 the *CPE* describes an ideal capacitor, when n ranges from 0.5 to 1.0 the *CPE* describes a distribution of dielectric relaxation times in frequency space, and when n is equal to 0.5 the *CPE* represents a Warburg impedance with diffusional character. From de n_{ct} values it can be seen that in the absence of inhibitor the corrosion process is controlled by charge transfer ($n_{ct} > 0.8$), and in the presence of inhibitor, the charge transfer is limited by diffusional processes ($n_{ct} \rightarrow 0.5$). This is due to the presence of the inhibitor film formed on the surface of carbon steel. Furthermore, after 12 hours, n_f values are greater than 0.8 and tends to increase with time, i.e., approaching to the behavior of an ideal capacitor. The values of n_f indicate the high capacitance of the film inhibitor which limits the charge transfer processes and therefore increases the corrosion resistance of the carbon steel.

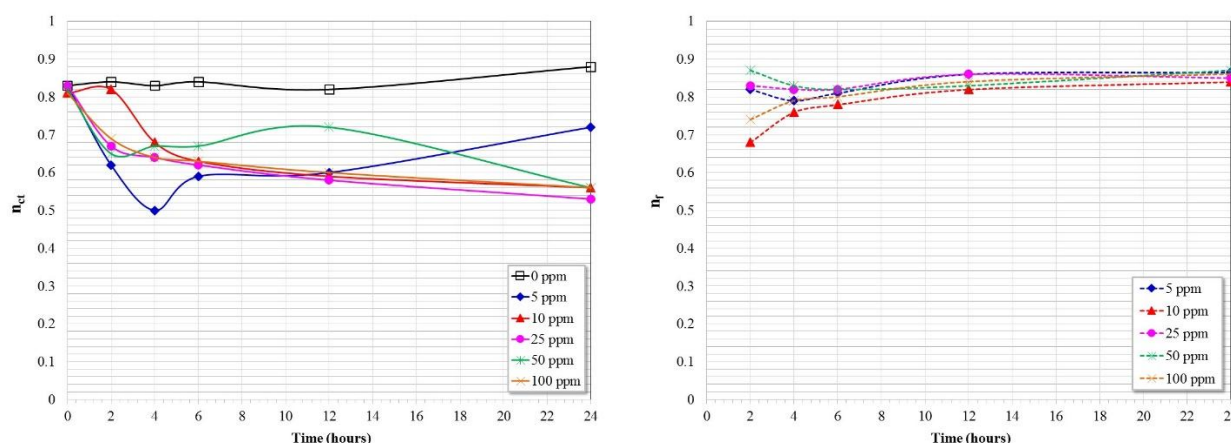


Figure 8. n_{ct} and n_f variation against time for carbon steel at different concentrations of coffee oil imidazoline.

Respect to Y_o , it is a proportional factor independent of the frequency which represents a combination of properties related both to the surfaces and the electroactive species, and when the value of n is equal to 1, Y_o is equal to the capacitance. Also Y_o is related to the time constant (τ_i) and the capacitance (C_i) of the *CPEs* according the following equations [32]:

$$\tau_i = (Y_{oi}R_i)^{1/n_i}$$

$$C_i = (Y_{oi}R_i^{(1-n_i)})^{1/n_i}$$

The capacitance of the associated capacitor is a measure of its capacity to store charge, and the time constant informs about the velocity of charge and discharge of the double electrochemical layer in the metal-solution interface, i.e., it is the time required for the return of the charge distribution to equilibrium after an electrical disturbance. On the basis of this equations, the double-layer capacitance (C_{dl}) and the capacitance of the film (C_f), well as the values of \square_{dl} and \square_f involved in the two *CPEs* (CPE_{dl} and CPE_f), of the equivalent circuits shown in Figure 6 can be calculated.

Figure 9 shows plots of the capacitance versus time for carbon steel at different concentrations of coffee oil imidazoline. For metal electrodes without inhibitor-film, the diameter of the high-

frequency semicircle is treated as the charge transfer resistance R_{ct} . However, for electrodes with inhibitor-film, the high frequency capacitive loop is related to the barrier and properties of the inhibitor layer [5]. From this viewpoint, in Figure 9 can be seen that the capacitance (C_{dl}) of the carbon steel without the presence of inhibitor shows a steady increase in their values as time elapsed. However, in those areas unprotected by the inhibitor (porous inhibitor film) its capacitance is greater than that of carbon steel without addition of inhibitor, and it tends to a constant value, except with the addition of 5 ppm of inhibitor. In this case the capacitance tends to that of carbon steel without the presence of inhibitor. This may be because the amount of inhibitor added is insufficient to protect the carbon steel surface. On the other hand, the capacitance values of the inhibitor film (C_f) are lower than those of carbon steel without addition of inhibitor, and their values tend to decrease as time passes. It is clear that the presence of inhibitor has a marked effect on the values of the capacitance. A decrease in the capacitance can happen if the inhibitor molecules (low dielectric constant) replace the adsorbed water molecules (high dielectric constant) on the carbon steel surface [33]. The capacitance is inversely proportional to the thickness of the double layer. Thus, decrease in the capacitance values could be attributed to the adsorption of the inhibitor on the metal surface. When the inhibitor is added into the electrolyte the active sites are covered by the inhibitor forming a smooth surface, consequently the capacitance decrease. In general, the surface area of a rough and porous electrode is large and the capacitance is high compared to that on a smooth surface. It has said that the imidazoline derivatives can be absorbed on the Fe surface through the imidazoline ring and heteroatoms, and the alkyl chain approximately perpendicular to the surface. Where the corrosion inhibition is achieved by the two factors; the exposed part of Fe surface is reduced by the covering of the imidazoline ring and heteroatoms, consequently preventing the surface from the water, and the alkyl chain (unpolar tail) prevents water molecules from contacting with the surface [34]. Therefore, with time, inhibitor molecules adsorb on the metal surface and the protective film grows until it covers all possible corroding sites by forming a thin mono-molecular film on the metal surface, hence reducing the capacitance values. The capacitance associated with the high-frequency time constant in presence of inhibitor was about 10^{-5} F/cm² or less after 24 hours of immersion.

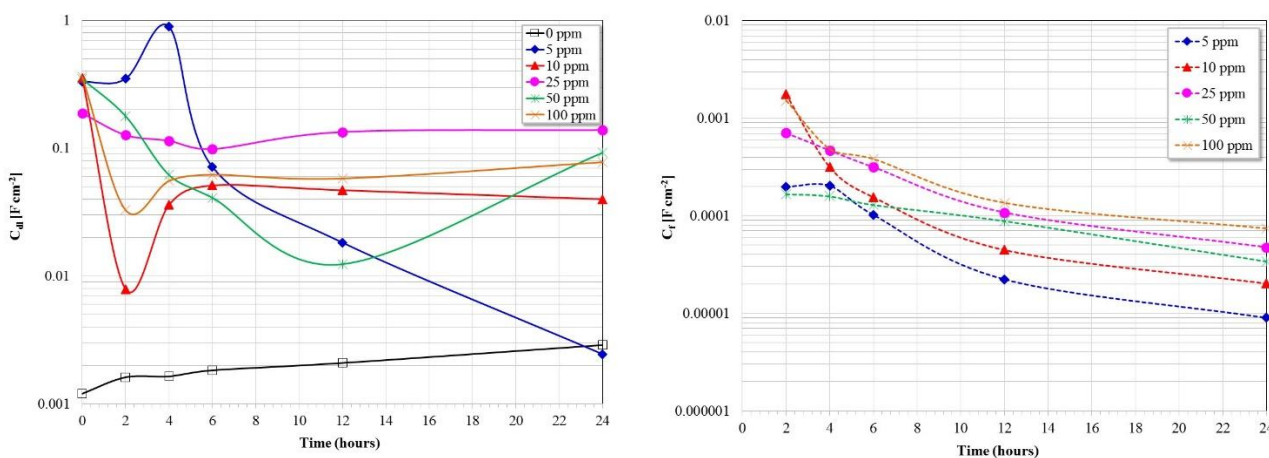


Figure 9. C_{dl} and C_f variation against time for carbon steel at different concentrations of coffee oil imidazoline.

If the adsorption of inhibitor molecules on the carbon steel surface decreases its electrical capacity because they displace the water molecules and other ions originally adsorbed on the surface, then the thickness of this protective layer can be estimated in accordance with Helmholtz model, given by the following equation [35, 36]:

$$C_f = \frac{\epsilon\epsilon_0}{d}$$

Where C_f is the capacitance per unit area, d is the thickness of the protective layer, ϵ is the dielectric constant of the protective layer and ϵ_0 is the permittivity of free space (8.8542×10^{-14} F cm⁻¹). In figure 10 the variation in the thickness of the protective film of inhibitor in function of time is showed. For the calculations a value of 30 for ϵ was used [37-39].

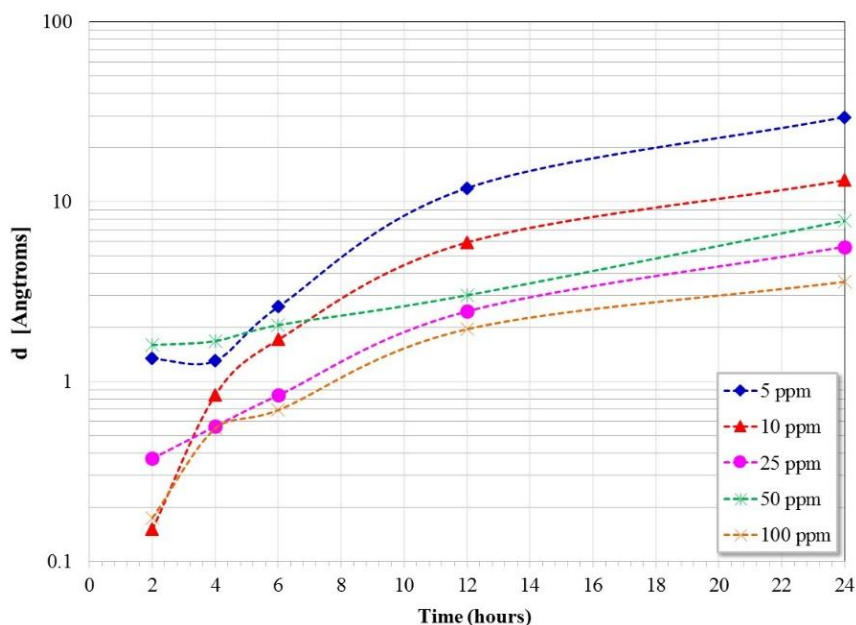


Figure 10. Variation of the thickness of the protective film of inhibitor against time for carbon steel at different concentrations of coffee oil imidazoline.

From this figure it can be observed that the maximum thickness of protective film is obtained at 5 and 10 ppm. However, according to the above discussion it is clear that the concentration of 5 ppm is not enough to form a protective film covering all the steel surface, and to concentrations greater than 10 ppm, the presence of excess inhibitor favors the appearance of electrostatic repulsion forces between the negative charges leading to a desorption of the inhibitor molecules, causing the appearance of unprotected sites on the metal and forming routes that led the pitting attack observed.

4. CONCLUSIONS

Electrochemical impedance spectroscopy (EIS) measurements have been carried out to study the performance of a new “green” oil-soluble inhibitor on the corrosion resistance of 1018 carbon

steel in in CO₂-saturated (3% NaCl + 10% diesel) emulsion at 50°C. The inhibitor under study was an imidazoline derivate based on coffee oil, where the coffee oil used for the synthesis of the inhibitor was extracted from coffee bagasse. EIS results have shown good inhibition properties of the hydroxyethyl-imidazoline derivate based on coffee oil, the optimal concentration is 10 ppm. The inhibitor decrease the corrosion rate by over 99.9%. Lower or higher concentrations than 10 ppm increases the corrosion rate because the surface area covered by the inhibitor decreases, either because the added concentration is not enough to form a protective film, or the presence of excess inhibitor favors the appearance of electrostatic repulsion forces between the negative charges leading to a desorption of the inhibitor molecules, causing the formation of unprotected sites on the metal. Therefore, the new inhibitor is a potential corrosion inhibitor for CO₂ corrosion on carbon steel in (3% NaCl + 10% diesel) emulsion.

Conflict Of Interest

The authors declare that there is no conflict of interests regarding the publication of this article

ACKNOWLEDGEMENTS

Financial support from Consejo Nacional de Ciencia y Tecnología (CONACYT, México) (Project 198687) is gratefully acknowledged.

References

1. X. Liu, P. C. Okafor, and Y. G. Zheng, *Corrosion Science*, 51 (2009) 744.
2. X. Liu, Y. G. Zheng, and P.C. Okafor, *Materials and Corrosion*, 60 (2009) 507.
3. W. Villamizar, M. Casales, L. Martinez, J. G. Chacon-Naca, and J. G. Gonzalez-Rodriguez, *Journal of Solid State Electrochemistry*, 12 (2008) 193.
4. W. Villamizar, M. Casales, J. G. Gonzalez-Rodriguez, and L. Martinez, *Journal of Solid State Electrochemistry*, 11 (2007) 619.
5. W. Villamizar, M. Casales, J. G. Gonzales-Rodriguez, and L. Martinez, *Materials and Corrosion*, 57 (2006) 696.
6. L. M. Rivera-Grau, M. Casales, I. Regla, D. M. Ortega-Toledo, J. G. Gonzalez-Rodriguez, and L. Martinez Gomez, *Int. J. Electrochem. Sci.*, 7 (2012) 13044.
7. L.M. Rivera-Grau, M. Casales, I. Regla, D.M. Ortega-Toledo, J.A. Ascencio-Gutierrez, J. Porcayo-Calderon, L. Martinez-Gomez, *Int. J. Electrochem. Sci.*, 8 (2013) 2491.
8. X. Zhang, F. Wang, Y. He, and Y. Du, *Corrosion Science*, 43 (2001) 1417.
9. F. Farelis and A. Ramirez, *Int. J. Electrochem. Sci.*, 5 (2010) 797.
10. Viswanathan S. Saji, *Recent Patents on Corrosion Science*, 1 (2011) 63.
11. V. Jovancicevic, S. Ramachandran, P. Prince, *Corrosion*, 55 (1999) 449.
12. U. Biermann W. Friedt, S. Lang, W. Lühs, G. Machmüller, J.O. Metzger, M.R. gen. Klaas, H.J. Schäfer, M.P. Schneider, *Angew. Chem. Int. Ed.*, 39 (2000) 2206–2224.
13. Lucas Montero de Espinosa, Michael A.R. Meier, *European Polymer Journal*, 47 (2011) 837–852.
14. M. Yadav, Sumit Kumar, P.N. Yadav, *Journal of Chemistry*, Volume 2013, Article ID 618684, 9 pages, <http://dx.doi.org/10.1155/2013/618684>.
15. Neha Patni, Shruti Agarwal, Pallav Shah, *Chinese Journal of Engineering*, Volume 2013, Article ID 784186, 10 pages, <http://dx.doi.org/10.1155/2013/784186>.

16. J.-M. Raquez, M. Deléglise, M.-F. Lacrampe, P. Krawczak, *Prog. Polym. Sci.*, 35 (2010) 487–509.
17. V. Sharma, P.P. Kundu, *Prog. Polym. Sci.*, 33 (2008) 1199–1215.
18. V. Sharma, P.P. Kundu, *Prog. Polym. Sci.*, 31 (2006) 983–1008.
19. J. Salimon, N. Salih, E. Yousif, *Arabian Journal of Chemistry*, 5 (2012) 135–145.
20. J.E.G. Gonzalez and J.C. Mirza-Rosca, *Journal of Electroanalytical Chemistry*, 471 (1999) 109.
21. J. Porcayo-Calderon, M. Casales-Diaz, L.M. Rivera-Grau, D.M. Ortega-Toledo, J.A. Ascencio-Gutierrez, L. Martinez-Gomez, *Journal of Chemistry*, 2014 (2014) 1.
22. D.M. Ortega-Sotelo, J.G. Gonzalez-Rodriguez, M.A. Neri-Flores, M. Casales, L. Martinez, A. Martinez-Villafañe, *Journal of Solid State Electrochemistry*, 15 (2011) 1997.
23. Li Yongjuan, Zhang Dun, Wu Jiajia, *Journal of Ocean University of China*, 9 (2010) 239.
24. Fei Kuang, Dun Zhang, Yongjuan Li, Yi Wan, Baorong Hou, *Journal of Solid State Electrochemistry*, 13 (2009) 385.
25. S. Tamilselvi, V. Raman, N. Rajendran, *Electrochimica Acta*, 52 (2006) 839.
26. S. Ramachandran, Bao-Liang Tsai, M. Blanco, H. Chen, Yongchun Tang, W.A. Goddard, *Langmuir*, 12 (1996) 6419.
27. S. O. Bondareva, V. V. Lisitskii, N. I. Yakovtseva, Y. I. Murinov, *Russian Chemical Bulletin*, 53 (2004) 803.
28. Y. van Ingelgem, A. Hubin, J. Vereecken, *Electrochimica Acta*, 52 (2007) 7642.
29. J.E. Ferrer, L. Victori, *Electrochimica Acta*, 39 (1994) 581.
30. L.D. Paolinelli, T. Perez, S.N. Simison, *Corrosion Science*, 50 (2008) 2456.
31. Houyi Ma, Xiaoliang Cheng, Guiqiu Li, Shenhao Chen, Zhenlan Quan, Shiyong Zhao, Lin Niu, *Corrosion Science*, 42 (2000) 1669.
32. Ahmed Y. Musa, Ramzi T.T. Jalgham, Abu Bakar Mohamad, *Corrosion Science*, 56 (2012) 176.
33. Shuwei Xia, Meng Qiu, Liangmin Yu, Fuguo Liu, Haizhou Zhao, *Corrosion Science*, 50 (2008) 2021.
34. C.H. Hsu, F. Mansfeld, *Corrosion*, 57 (2001) 747.
35. J.R. Scully, D.C. Silverman, M.W. Kendig (eds.). *Electrochemical Impedance: Analysis and Interpretation*, ASTM STP 1188, ASTM, Philadelphia, PA, 480 pp.
36. J. Liu, D.D. Macdonald, *Journal of the Electrochemical Society*, 148 (2001) B425.
37. Željka Petrović, Mirjana Metikoš-Huković, Robert Peter, Mladen Petravić, *Int. J. Electrochem. Sci.*, 7 (2012) 9232.
38. Željka Petrović, Mirjana Metikoš-Huković, Ranko Babić, *Electrochimica Acta*, 75 (2012) 406.